Reentrant condensation of DNA induced by multivalent counterions

T. T. Nguyen
Theoretical Physics Institute, University of Minnesota, 116 Church Street SE, Minneapolis, Minnesota 55455

I. Rouzina
Department of Biochemistry, University of Minnesota, 1479 Gortner Avenue, St. Paul, Minnesota 55108

B. I. Shklovskii
Theoretical Physics Institute, University of Minnesota, 116 Church Street SE, Minneapolis, Minnesota 55455

(Received 8 September 1999; accepted 3 November 1999)

A theory of condensation and resolubilization of a dilute DNA solution with growing concentration of multivalent cations, N, is suggested. It is based on a new theory of screening of a macroion by multivalent cations, which shows that due to strong cation correlations at the surface of DNA the net charge of DNA changes sign at some small concentration of cations N_0. DNA condensation takes place in the vicinity of N_0, where absolute value of the DNA net charge is small and the correlation induced short range attraction dominates the Coulomb repulsion. At $N>N_0$ positive DNA should move in the opposite direction in an electrophoresis experiment. From comparison of our theory with experimental values of condensation and resolubilization thresholds for DNA solution containing Spe^{4+}, we obtain that $N_0=3.2$ mM and that the energy of DNA condensation per nucleotide is 0.07 k_BT. © *2000 American Institute of Physics.* [S0021-9606(00)51305-1]

I. INTRODUCTION

In the last several years there has been a revival of interest in the phenomenon of DNA condensation with multivalent cations. The reason for this interest is the general effort of the scientific community to develop effective ways of gene delivery for the rapidly growing field of genetic therapy. The DNA compaction should be fast, effective, easily reversible and should not damage the DNA double helix. All of these conditions are fulfilled in DNA condensation with multivalent cations, such as $CoHex^{3+}$, naturally occurring polyamines Spd^{3+}, Spe^{4+} and their analogs which are known to bind to DNA in the predominantly nonspecific electrostatic manner. The DNA condensates obtained this way are indeed closely packed arrays of parallel DNA strands. It was shown that the helical structure of the B-DNA is not perturbed within such condensate, and that the reaction is easily reversed by the addition of monovalent salt, or simply dilution of the solution with water. Cations with larger and more compact charge are more effective in condensing the DNA. This also suggests an electrostatic mechanism of the DNA condensation with multivalent cations. During about 20 years of research, a significant amount of information on DNA condensation has been accumulated. For long DNA, as the concentration of Z-valent cations grows condensation happens abruptly at some critical concentration, N_c which depends on the charge of cations and the concentration of monovalent salt n. A comprehensive review of the experimental and theoretical results for N_c can be found in Refs. 1, 2.

The intensive study of the last few years revealed completely new features of DNA condensation with multivalent cations.[3–6] It was discovered that when the concentration of cations grows far beyond N_c to some new critical value $N_d \gg N_c$, DNA dissolves and returns to the solution. This reentrant condensation behavior is schematically shown in Fig. 1. For a long DNA and small n both transitions are very sharpand the ratio of N_d/N_c can be as large as 10^4. Remarkably, the decondensation threshold N_d is almost totally independent on the monovalent salt concentration, n. On the other hand, the condensation threshold, N_c, grows with increasing n.

It has been understood for some time that, due to correlations between multivalent cations at the DNA surface,[7–15] two DNA molecules experience a short range attraction, which can lead to condensation. Monovalent ions are much less correlated and do not provide any attraction. Conventional explanation for the condensation threshold N_c is that it is just the bulk concentration of Z-valent cations, $N=N_r$, at which they replace monovalent ones and begin to produce a short range attraction. However, from this point of view it is very difficult to understand why at large $N=N_d$, DNA molecules go back to the solution.

The above explanation also does not take into account the net charge of DNA. The nonlinear Poisson–Boltzmann equation predicts[18,19] a value for the net linear charge density of DNA, η^*, which includes the bare charge of DNA and the charge of cations bound at the very surface of DNA with energy larger than k_BT. This charge is negative and does not depend on N. At $N>N_r$, two situations are possible. The energy of the Coulomb repulsion can be smaller than the energy of the short range attraction. Then DNA condenses at $N=N_r$ but never dissolves back. If the energy of the Coulomb repulsion is larger than the energy of short range attraction, condensation does not happen at all. Both possibilities contradict experiments and therefore reentrant condensation cannot be explained in the Poisson–Boltzmann approximation.

In this paper we propose an explanation for the reentrant

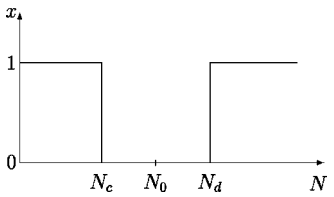

FIG. 1. Schematical illustration of the reentrant condensation. The fraction x of DNA molecules in solution is plotted as a function of logarithm of the cation concentration.

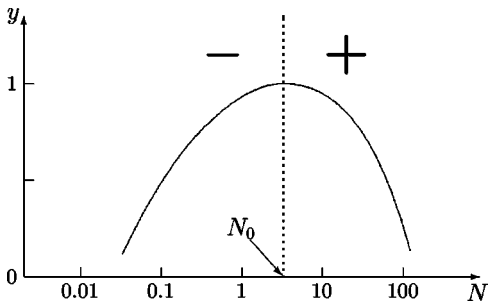

FIG. 2. Phase diagram of a dilute DNA solution in the plane of the bulk cation concentration N (in units of mM) and variable y defined by Eq. (1). The solid curve was plotted using Eq. (23) with fitting parameters obtained from the data (Ref. 3) for long DNA screened by Spe^{4+}. Above the curve, all DNA molecules are in solution ($x=1$). Below the solid curve, the segregation domain is located. Here the condensed phase of DNA appears and in regions far enough from the curve, it consumes most of DNA ($x \ll 1$). The dotted line corresponds to $N=N_0$, where the net charge of DNA changes sign from negative to positive.

condensation based on a new theory of screening of macroions by multivalent cations, which emphasizes the strong correlations of multivalent cations at the surface of DNA. We explain why the condensed phase exists only within the limited range, $N_c \leqslant N \leqslant N_d$ and calculate both N_c and N_d.

It was shown in Refs. 16, 17, that the strong repulsion between multivalent cations leads to their strong lateral correlations. The resulting strongly correlated liquid of multivalent cations at the surface of DNA has a large negative chemical potential, μ, which describes the additional purely electrostatic binding of cations to the surface ($|\mu| \gg k_BT$). This, in turn, leads to an exponentially small concentration of cations above the surface, $N_0 = N_s \exp(-|\mu|/k_BT)$, where N_s is the concentration of counterions within the condensed layer. The concentration N_0 can be still larger than N_r, if n is not unrealistically large.

According to Refs. 16, 17, when the bulk concentrations of multivalent cations, N, grows above N_r, the net negative charge η^* decreases in absolute value and crosses zero at $N=N_0$. At $N>N_0$, the net charge becomes *positive* and continues to grow with N. This effect is called charge inversion. It is worth noting here that the charge inversion is not a result of some specific chemosorbtion,[20] but rather a direct consequence of purely electrostatic interactions of multivalent cations.

At $N=N_0$ there is no Coulomb repulsion at all, so that the short range attraction dominates and leads to condensation. This is actually the optimal situation for condensation. It is obvious that there is a range of N around N_0 where attraction still dominates and DNA condenses. Condensation thresholds N_c and N_d then are determined by the condition that the energy of the short range attraction is equal to the energy of Coulomb repulsion of negative and positive DNA molecules, respectively. This means that the concentration N_0 is located inside the window $N_c \leqslant N \leqslant N_d$ (see Fig. 1) and the width of the window grows with the strength of the short range attraction.

Below we present an analytical theory, which calculates both critical concentrations N_c and N_d in terms of the two main physical parameters of the system: boundary concentration of multivalent cations N_0 and the energy, ε, of the DNA binding within the DNA bundle per nucleotide.

At a small concentration of monovalent salt, n, the condensation threshold N_c calculated in our theory is larger than the replacement concentration N_r. This means that the replacement of monovalent cations happens before the condensation and by itself cannot lead to the condensation while Coulomb forces are still strong. On the other hand, if n is so large that N_r is larger than the calculated N_c (which assumes that replacement has happened), the condensation actually happens only at $N=N_r$. Thus, a large concentration of monovalent ions, n, acts as a ''curtain.'' It eliminates a part of the window predicted by our theory. We show below that in the experiment of Ref. 3 the ''curtain effect'' starts to work only at $n>50$ mM.

Two central parameters of our theory, N_0 and ε, can be calculated for a simple model of DNA as a uniformly charged cylinder.[15–17] They can be also directly measured in independent experiments. The energy ε was measured in Ref. 21.

On the other hand, one can obtain these parameters from the experimental values of N_c and N_d. Below we use condensation and resolubilization for DNA with Spe^{4+} to estimate ε and N_0. We obtain $\varepsilon = 0.07\ k_BT$ and $N_0 = 3.2$ mM. The first number reasonably agrees with experimental data.[21]

Thus far we have talked about long DNA. For short DNA fragments, one should take into account the mixing entropy of DNA molecules which makes their solution more stable and makes the window between N_c and N_d smaller. We calculate the phase diagram for the condensation of DNA olygomers consisting of L/b bases (L is the length of olygomer, $b=1.7$ Å is length of double helix per phosphate). This phase diagram is shown in Fig. 2 on the plane (N,y), where

$$y = \frac{k_BTb}{\varepsilon L} \ln \frac{C_{\max}}{C}, \tag{1}$$

C is the concentration of DNA molecules and $C_{\max}$ is its maximum value (equal to the inverse volume of a DNA molecule). Below the solid curve, in segregation domain, condensed and dissolved phases coexist. Thinking about very small concentrations of DNA, $C \ll C_{\max}$, we completely ignore the lower border of the segregation domain. Above the solid curve, all DNA molecules are in solution. A solution of long DNA molecules corresponds to a horizontal line $y = y_0 \ll 1$. As concentration of DNA or its length decreases, the window between N_c and N_d shrinks. Condensation provides largest gain of free energy at $N=N_0$ where DNA mol-

ecules are neutral. This is why the phase boundary curve peaks at $N=N_0$. The dotted line, $N=N_0$, on Fig. 2 divides the plane in two parts. At $N<N_0$ the net charge of a DNA molecule is negative, while at $N>N_0$ it is positive. This net charge by definition includes cations which are bound to DNA with binding energy larger than k_BT. Therefore, they move together with DNA in gel electrophoresis. This means that DNA should move in the direction opposite to the conventional one if $N>N_0$.[17] It would be interesting to verify this prediction experimentally. We propose also to combine experimental study of the condensation phase diagram with the gel electrophoretic measurement of the charge on the dissolved DNA molecules.

II. CRITERION OF EQUILIBRIUM BETWEEN CONDENSED AND DISSOLVED PHASES OF LONG DNA

In this section we consider long DNA molecules in an aqueous solution containing Z-valent counterions of the bulk concentration N. DNA condensation and resolubilization take place when the chemical potential of DNA in its condensed and dissolved states are equal, i.e.,

$$\mu_c=\mu_d. \tag{2}$$

For a long DNA we can neglect the entropy of DNA in both phases. We view the condensed phase as a bundle of parallel molecules which stick together due to correlation induced short range attraction to the nearest neighbors. The chemical potential of DNA molecule in the condensed phase in this approximation is determined by

$$\mu_c=-\varepsilon L/b, \tag{3}$$

where L/b is the number of negative charges in a DNA molecule.

Each molecule of a large bundle is practically neutral. More exactly its charge is inversely proportional to the number of molecules in the bundle.[15] This happens because the total charge of a large bundle keeps counterions inside the bundle very effectively.

On the other hand, in the dissolved state, each molecule acquires finite net charge density, η^*. This happens because a finite fraction of its counterions moves to the Debye–Hückel atmosphere in order to increase their entropy. One can view a single DNA molecule and its Debye–Hückel atmosphere as a cylindrical capacitor with linear charge densities η^* (inside) and $-\eta^*$ (outside). We recall that the net linear charge density of DNA, η^*, includes the bare charge and the charge of cations residing at the very surface of DNA and attached to the surface with binding energy larger than k_BT.

In equilibrium the electrostatic potential on the surface of DNA, φ_0, is determined by the ratio of the cation concentration in the bulk, N and the concentration near the surface of DNA, N_0:

$$Ze\varphi_0=-k_BT\ln\frac{N_0}{N}. \tag{4}$$

This potential acts like a voltage difference applied to the capacitor.

The free energy per DNA molecule or the chemical potential of the dissolved phase can be written as

$$\mu_d=-\tfrac{1}{2}\varphi_0\eta^*L. \tag{5}$$

To derive Eq. (5) one should add the energy of the electric field of the capacitor,

$$U=\tfrac{1}{2}\varphi_0\eta^*L, \tag{6}$$

to the change of the entropy term of the free energy of cations when they move from the surface of DNA to the bulk of solution

$$\frac{L\eta^*}{Ze}k_BT\ln\frac{N_0}{N}=-\varphi_0\eta^*L \tag{7}$$

[here Eq. (4) was used]. Equivalent derivation can be found, for example, in Ref. 22. Comparing Eq. (5) and Eq. (6) we see that the change of the free energy of the capacitor is equal to the energy of an electric field with a minus sign. This is a realization of the general theorem valid for any capacitor kept at constant voltage.[23]

The surface potential, φ_0, can be easily related to the net charge density η^*. Indeed, at distance r from its surface, a cylinder of radius a and linear charge η^* creates a potential

$$\varphi(r)=\varphi_0-\frac{2\eta^*}{D}\ln\left(\frac{a+r}{a}\right), \tag{8}$$

where D is the dielectric constant of water. This potential vanishes beyond the Debye screening length,

$$r_s=(4\pi l_B)^{-1/2}(NZ^2+ZN+2n)^{-1/2}, \tag{9}$$

where $l_B=e^2/Dk_BT$ is the Bjerrum length. Therefore, substituting $r=r_s$ and $\varphi(r_s)=0$ into Eq. (8) one obtains

$$\varphi_0=\frac{2\eta^*}{D}\ln\left(\frac{a+r_s}{a}\right). \tag{10}$$

Substituting Eq. (10) into Eq. (5) we get

$$\mu_d=-\frac{(\eta^*)^2}{D}L\ln(1+r_s/a). \tag{11}$$

Using the condition Eq. (2) together with the expressions for the chemical potentials for both states, Eqs. (3) and (11), we arrive at the final equation for the DNA reentrant condensation transitions

$$\frac{\varepsilon}{k_BT}=\frac{b(\eta^*)^2}{D}\ln(1+r_s/a). \tag{12}$$

To proceed further one has to know the net charge density, η^*. The next section gives a review of current understanding of this quantity.

III. NET LINEAR CHARGE DENSITY OF SCREENED DNA

Conventional understanding of nonlinear screening of a strongly charged cylinder is based on the Poisson–Boltzmann equation. Let us first consider a cylinder with a negative bare linear charge density, $-\eta$, which is screened by Z-valent cations ($n=0$). Assume that $\eta>\eta_c$, where $\eta_c=e/l_B$ ($\eta=4.2\ \eta_c$ for double helix DNA). Onsager and

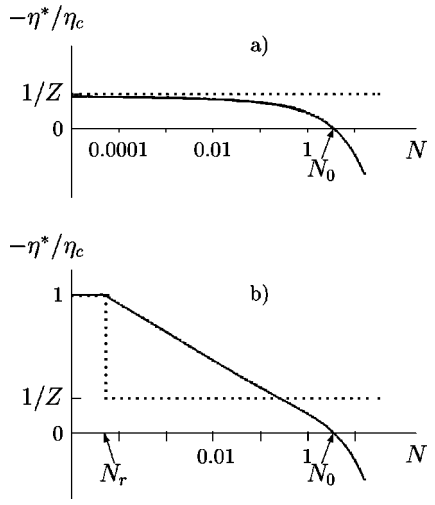

FIG. 3. The dimensionless net linear charge density η^*/η_c as function of Z-valent cation concentration N (in units of mM) at zero concentration n of monovalent salt (a) and at finite n (b). The solid curves are drawn according Eq. (13) with parameters obtained from the data (Ref. 3) for DNA screened by Spe^{4+}. Dotted curves represent conventional understanding of results of the Poisson–Bolzmann equation. N_0 is the concentration of Z-valent ions at the surface of DNA and N_r is the concentration N at which Z-valent cations replace monovalent ones.

Manning[18] argued that such a cylinder is partially screened by counterions residing at the very surface, so that the net linear charge density of the cylinder, η^*, is equal to the negative universal value $-\eta_c/Z$. The rest of the cylinder charge is linearly screened at much larger distances according to the linear Debye–Hückel theory. The net charge, η^*, does not depend on the bulk concentration of cations, N and is shown (in units of $-\eta_c$) by the dotted line on Fig. 3(a). The Onsager–Manning picture of condensation was confirmed by the solution of the Poisson–Boltzmann equation.[19]

Let us now discuss a water solution, containing both a concentration, n, of monovalent salt and a concentration, N of Z:1, salt. When N grows to some well defined concentration, $N=N_r$, multivalent cations replace monovalent ones at the surface of DNA. According to conventional understanding[24,25] this replacement of the condensed monovalent ions changes $-\eta^*/\eta_c$ from 1 to $1/Z$ [see the dotted line on Fig. 3(b)]. In logarithmic scale this transition looks quite abrupt.

In recent papers[16,17] the influence of strong correlations of multivalent cations at the surface of a macroion on its net charge, η^*, was studied. The general expression for the net linear charge density, η^*, was derived:

$$\eta^* = -\frac{\eta_c}{2Z}\frac{\ln(N_0/N)}{\ln(1+r_s/a)}. \tag{13}$$

This equation takes into account correlations with the help of the new boundary condition $N(r=0)=N_0$ for the Poisson–Boltzmann equation. To remind derivation of this result let us write down the Boltzmann formula

$$N(r) = N_0 \exp\left(-\frac{Ze}{k_BT}(\varphi(r)-\varphi_0)\right), \tag{14}$$

At $r=r_s$ the concentration $N(r)$ reaches its bulk value, N. Substituting Eq. (10) into Eq. (14) we obtain

$$N = N_0 \exp\left(\frac{2Z\eta^*}{\eta_c}\ln\left(\frac{a+r_s}{a}\right)\right). \tag{15}$$

Expressing η^* in terms of the bulk cation concentration N we arrive at Eq. (13). This equation was used to plot solid lines on Fig. 3.

At $n=0$ [Fig. 3(a)] one can see[17] that Manning's limiting value of $\eta^*=-\eta_c/Z$ holds only for the unrealistically small N. At larger N the absolute value of the net charge decreases, η^* crosses zero and becomes positive.

At finite n, the screening radius, r_s, strongly decreases and at small N the net charge density, $-\eta^*$, becomes larger than η_c/Z [see solid line on Fig. 3(b)]. It was shown in Ref. 17 that when N goes to N_r, the density η^* becomes as large as η_c, so that at the replacement point the net density, η^*, matches its standard value for monovalent ions. At larger N the role of the monovalent salt is smaller and η^* is similar to that of $n=0$. The density, η^*, crosses zero at $N=N_0$ and becomes positive. In the next section we will use Eq. (13) to find the condensation and resolubilization thresholds.

IV. REENTRANT CONDENSATION THRESHOLDS FOR LONG DNA MOLECULES. COMPARISON WITH EXPERIMENT

Now we can substitute Eq. (13) into Eq. (12) and obtain an explicit equation for the threshold concentrations:

$$\frac{\varepsilon}{k_BT} = \frac{1}{4Z^2\xi}\frac{\ln^2(N_0/N)}{\ln(1+r_s/a)}. \tag{16}$$

Here $\xi=l_B/b$ is the conventional Manning's parameter ($\xi=4.2$ for DNA). Obviously, there exist two solutions, N_c and N_d, for the bulk concentration, N, which corresponds, respectively, to the condensation and dissolution transition points.

Concentration N_c is usually so small that r_s is dominated by monovalent ions and $r_s=r_1=(8\pi l_B n)^{-1/2}$. With the help of Eq. (16) we arrive at a simple equation for N_c:

$$\frac{\varepsilon}{k_BT} = \frac{1}{4Z^2\xi}\frac{\ln^2(N_0/N_c)}{\ln(1+r_1/a)}. \tag{17}$$

To obtain an equation for N_d, we take into account that in the case of Spe^{4+} cation,[3] the condensed phase dissolves at $N_d \approx 150$ mM. At such a large concentration of Z:1 salt we can neglect the monovalent salt concentration n in Eq. (9). Even then according to Eq. (9) screening radius r_s turns out to be 0.2 nm, much smaller than the average distance between anions in the bulk of solution, $(NZ)^{-1/3}=1.3$ nm. This means that the Debye–Hückel theory does not work even in the bulk. Strictly speaking for such large N our theory as well as results of Refs. 15–17 should be modified. Two correlation effects should be considered in such a nonideal plasma.

First, strong repulsive correlations between cations can substantially increase r_s. Role of these correlations can be illustrated qualitatively assuming that anions form a uniform background and cations are pointlike particles or, in other

words, using a concept of one-component plasma (OCP). For such a model, role of cation correlations depends on the parameter $\Gamma=(Ze)^2/(Dr_N k_B T)$, where $r_N=(4\pi N/3)^{-1/3}$. Debye–Hückel theory works only for $\Gamma \ll 1$. At $Z=4$ and $N=N_d=150$ mM one finds that $\Gamma \approx 8$. At such Γ thermodynamic properties of OCP are closer to that of Wigner crystal than to the ideal gas. In particular compressibility of OCP becomes negative. This dramatically changes the character of screening by Z:1 salt. In the sum on the right side of Eq. (9) the large positive term NZ^2 gets replaced by a *negative* value describing contribution of OCP. Thus, r_s becomes even larger than $r_s=0.5$ nm which Debye–Hückel theory gives when only anions are taken into account. Note that cations Spd^{3+} and Spe^{4+} are 1.5 and 2 nm long polymers, not pointlike ions. Therefore, application of OCP can be considered as a crude illustration only.

Second, monovalent anions can be incompletely dissociated from *Z*-valent cations. This effect is not very strong for cations Spd^{3+} and Spe^{4+} because they are quite large. Still it can substantially increase r_s. For the purpose of a crude estimate we assume that r_s is of the order of average distance between anions $d=(N_d Z)^{-1/3}=1.3$ nm at $N=N_d$. Then equation for N_d has a form

$$\frac{\varepsilon}{k_B T}=\frac{1}{4Z^2\xi}\frac{\ln^2(N_0/N_d)}{\ln(1+d/a)}. \tag{18}$$

The same two correlations effects lead to another revision of our theory. Strictly speaking in the numerator of the right side of Eq. (18) the concentration of cations N should be replaced by its active fraction N^{act}, which can be substantially smaller than N. We could not find values of N^{act} for such large concentrations N of Spd^{3+} or Spe^{4+} in the literature. Therefore, for the purpose of estimate, we proceed using N_d instead of N_d^{act}.

In practice, the concentrations N_c and N_d are known from experiments, so that important parameters ε and N_0 can be found with the help of Eqs. (17) and (18). For example, N_0 can be found by eliminating ε from Eqs. (17), (18). In the specific experimental situation of Ref. 3 where long DNA molecules condensed with a 4-valent cation, Spe^{4+}, $N_c=0.025$ mM and $N_d=150$ mM at the lowest concentration $n=10$ mM of NaCl. Using these values we obtain from Eqs. (17), (18) $N_0=3.2$ mM and $\varepsilon/k_B T\approx 0.07$. The last value favorably agrees with the energy of attraction between the Co-Hex condensed DNA obtained in the osmotic stress experiment,[21] $\varepsilon=0.08\ k_B T$.

Knowing N_0 and ε, we can try to reproduce the experimental dependence of the condensation threshold N_c on concentration of NaCl, obtained in Ref. 3. This can be done with the help of Eq. (17):

$$\ln N_c=\ln N_0-\left(4Z^2\xi\frac{\varepsilon}{k_B T}\ln(1+r_1/a)\right)^{1/2}. \tag{19}$$

The calculated function $N_c(n)$ is shown in Fig. 4 together with the experimental points from Ref. 3. It is clear that Eq. (19) closely reproduces experimental behavior until $n \lesssim 50$ mM. The later value is close to the concentration of monovalent cations which is needed to replace 4-valent cations at the surface of DNA for $N\approx 0.01$ mM. It seems that at

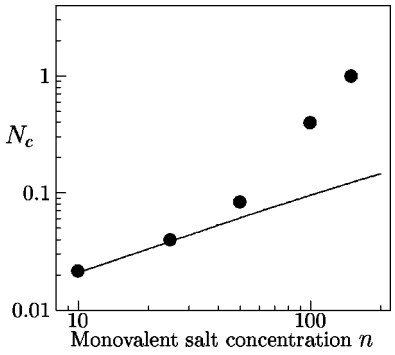

FIG. 4. The condensation threshold N_c (in unit of mM) as a function of monovalent salt concentration, n. The solid curve corresponds to Eq. (19). Experimental data (Ref. 3) are shown by the large dots.

$n>50$ mM, condensation happens simultaneously with the replacement of monovalent cations by multivalent ones, i.e., at $N_c\sim N_r$, as was assumed in Ref. 25.

We would like to emphasize that at low monovalent salt concentrations $n<50$ mM, there is a broad range of concentrations $N_c>N>N_r$ in which multivalent cations cover the DNA surface, but condensation does not happen. In this range, the Coulomb repulsion of negative DNA molecules is strong enough to prevent condensation because, as shown in Fig. 3(b), the absolute value of the net negative charge on the polymer, $-\eta^*$, does not abruptly decrease from η_c to η_c/Z at $N_c\sim N_r$, but still stays larger than η_c/Z in the large interval of $N>N_r$.

In contrast with N_c, the resolubilization threshold N_d practically does not depend on n. This happens because at $N=N_d$, screening is dominated by multivalent cations and agrees with our Eq. (18).

Let us now discuss another experimental study[4] in which DNA solution was condensed with trivalent Spd^{3+} cations. In this case, for $n=4$ mM, the threshold concentrations equal $N_c\approx 2$ mM and $N_d\approx 60$ mM, which yields $N_0\approx 11$ mM and $\varepsilon/k_B T\approx 0.02$. This value of $\varepsilon/k_B T$ is about three times smaller than for Spe^{4+}. This is quite reasonable, if attraction has an electrostatic nature.

The concentrations, N_0, we obtained above, are substantially larger than concentrations 0.3 mM and 1 μM predicted by the microscopic theory[17] for the pointlike 3- and 4-valent cations, respectively. This can be related to approximations made both in theoretical calculation of N_0 and in the above procedure of extraction of N_0 from the experimental data.

On the theoretical side, as we mentioned above, cations Spd^{3+} and Spe^{4+} are quite long linear polymers (1.5 and 2.0 nm, respectively). Their length is approximately equal to the average distance between cation centers in two-dimensional strongly correlated liquid of cations on the surface of DNA. As a result $|\mu|$ can be smaller for Spd^{3+} and Spe^{4+} than for pointlike ions, what in turn can lead to exponential growth of N_0. Thus, to obtain a more reliable theoretical prediction of N_0, one has to study the thermodynamic properties of the strongly correlated (possibly nematic) liquid of these ions on an uniform negative background by numerical methods.

On the experimental side, in the correct procedure one should replace N_d by N_d^{act}. This can lead to substantial de-

crease of experimental value of N_0. As we saw above, N_0 is extremely important parameter which can be used in many experimental situations. Therefore, we suggest to study activity of Spd^{3+} and Spe^{4+} in the vicinity of 100 mM to correct the experimental values of N_0.

Note that Ref. 3 also contains information on the single and triple stranded DNA helices, which condensed in the narrower and wider range of $[Spe^{4+}]$ than the double helices, respectively. This tendency agrees with idea that correlations play the major role in this phenomenon.

Concluding our discussion, we would like to emphasize that there is another reason why application of our theory to the experimental data[3,4] is not completely convincing. Indeed, our theory assumes that that the concentration of DNA phosphates N_{ph} is smaller than N, so that the DNA charge can be easily compensated by Z-valent cations. Actually in experimental conditions[3,4] the condensation threshold N_c happens to be close to N_{ph}. This situation deserves special theoretical treatment which will be a subject of a future work. For more reliable comparison with the theory of this paper we need experiments at smaller concentrations of DNA phosphates.

V. CONDENSATION OF SHORT DNA MOLECULES

In this section we explicitly deal with the mixing entropy of DNA molecules in the dissolved state, and calculate the phase diagram for the DNA solution. We consider double helix DNA molecules of length L, with L/b bases each.

The free energy per DNA molecule in solution with concentration C is

$$F=-xk_BT\left(\ln\left(\frac{C_{\max}}{Cx}\right)+1\right)-(1-x)\frac{L}{b}\Delta, \tag{20}$$

where $1-x$ is the fraction of DNA molecules in the condensate. The first term in Eq. (20) is the entropy of the dissolved DNA phase per molecule of DNA. Here $C_{\max}\sim 1/\pi a^2 L$ is the inverse volume of the DNA molecule. The second term in Eq. (20) is the average free energy per molecule in the condensed state. Here Δ is the difference between the energy of short range attraction ε and the free energy $b\mu_d/L$ of the screening atmosphere per nucleotide [see Eq. (11)]:

$$\frac{\Delta}{k_BT}=\frac{\varepsilon}{k_BT}-\frac{1}{4Z^2\xi}\frac{\ln^2(N_0/N)}{\ln(1+r_s/a)}. \tag{21}$$

Minimizing Eq. (20) with respect to x, we find

$$x=\frac{C_{\max}}{C}\exp\left(-\frac{\Delta}{k_BT}\frac{L}{b}\right). \tag{22}$$

Then the boundary of two-phase domain $x=1$ corresponds to the condition

$$\frac{k_BTb}{\varepsilon L}\ln\frac{C_{\max}}{C}=1-\frac{k_BT}{4Z^2\xi\varepsilon}\frac{\ln^2(N_0/N)}{\ln(1+r_s/a)}, \tag{23}$$

Eq. (23) specifies the conditions when the chemical potentials of the condensed and dissolved states of DNA are equal. The curve described by Eq. (23) forms a boundary on the phase diagram on Fig. 2, separating the region of the dissolved DNA (above it) from the region where the condensed and dissolved phases of DNA coexist (below it). Within the separation domain the fraction of dissolved DNA is given by Eq. (22).

The dotted line $N=N_0$ divides the phase diagram of Fig. 2 into two regions where the DNA molecules have opposite signs. Positive net charge of dissolved DNA can be measured in an electrophoresis experiment because cations included in this charge are bound to DNA with a binding energy larger than k_BT and therefore move together with DNA molecule. At $N>N_0$ one should see that DNA molecules are positive both above and below phase boundary of Fig. 2. However, below the boundary, intensity of corresponding electrophoresis peak should decay rapidly with the distance from the boundary. This intensity is picked up by slowly moving bundles of DNA molecules, which at large enough N can be also positive.

The position and the shape of the phase boundary obviously depends on the values of the parameters N_0, ε/k_BT and $2Z^2\xi$. For double-helix DNA with Spe^{4+} we find $2Z^2\xi=134$. Using the estimates $\varepsilon/k_BT=0.07$ and $N_0\approx 3.2$ mM obtained above we can calculate the phase boundary for condensation of the DNA fragments of the arbitrary length if we know r_s as function of N. Because of poor understanding of screening at large N (see above) we do not have such a general expression for r_s. Therefore, only for an illustration, we plotted the phase diagram on Fig. 2 using $r_s=r_1$ for $N<N_0$ and $r_s=(NZ)^{-1/3}$ at $N>N_0$.

VI. CONCLUSION

The theory of DNA condensation and resolubilization by multivalent cations presented above makes several novel, well defined predictions which have not been confirmed by experiment yet. The main results of the study are summarized in the phase diagram presented in Fig. 2. There are only two physical parameters ε and N_0 on which the shape of the phase boundary depends. Therefore measuring just a few threshold concentrations of multivalent cations N_c and N_d for solution of DNA fragments of different length and/or concentrations should yield several independent determinations of these quantities, and at the same time provide the test for the self-consistency of our model. Experimental studies of DNA phase diagram with different multivalent cations would provide the values of the attractive energy for different ions. In the present theory the origin of parameters ε and N_0 was not specified and they were treated as phenomenological parameters. Comparison of experimentally determined ε and N_0 values for different counterions should yield information about the nature of the attraction. It is worth noting here that the value of ε is determined by the balance of the attraction due to the correlations of multivalent cations with all of the repulsive non-Coulomb DNA–DNA interaction. The first interaction decays with DNA–DNA distance slower than the second one. Then the binding energy ε is determined by correlations. In this case, the two quantities ε and N_0 are not independent[15,17] namely $\ln N_0 \propto \varepsilon$. For the model of the uniformly charged cylinder and pointlike cations both parameters were calculated microscopically.[15,17]

We would like to emphasize that the concentration N_0 found in this paper plays extremely important role in any phenomenon related to screening of DNA molecules by multivalent ions.[16,17] In this paper, we try to attract attention to the fact that N_0 plays major role in electrophoresis, because the net linear charge density of DNA η^* changes sign at $N=N_0$. It was predicted[16,17] that DNA should start moving in the opposite direction at $N>N_0$. It is not obvious that one can see this phenomenon for long DNA. Indeed, in large interval of concentrations $N_0<N<N_d$ most of long DNA molecules are condensed in low mobility bundles while concentrations $N>N_d$ may be difficult for experiment because of large dissipation of heat. To avoid this problem, we suggest doing electrophoresis of a solution of short DNA fragments. In this case all DNA molecules have unconventional sign of mobility at concentrations smaller than N_d. The phase diagram shown in Fig. 2 predicts good conditions for such an experiment. It would be very interesting to verify predicted correlations between the reentrant condensation and unconventional electrophoresis.

ACKNOWLEDGMENTS

We are grateful to A. Yu. Grosberg, V. A. Bloomfield and R. Podgornik for valuable discussions. This work was supported by NSF DMR-9616880 (T. N. and B.S) and NIH GM 28093 (I. R.).

[1] V. A. Bloomfield, Curr. Opin. Struct. Biol. **6**, 334 (1996).
[2] V. A. Bloomfield, Biopolymers **44**, 269 (1998).
[3] M. Saminathan, T. Antony, A. Shirahata, L. Sigal, T. Thomas, and T. J. Thomas, Biochemistry **38**, 3821 (1999).
[4] J. Pelta, D. Durand, J. Doucet, and F. Livolant, Biophys. J. **71**, 48 (1996).
[5] J. Pelta, F. Livolant, and J.-L. Sikorav, J. Biol. Chem. **271**, 5656 (1996).
[6] E. Raspaud, M. Olvera de la Cruz, J.-L. Sikorav, and F. Livolant, Biophys. J. **74**, 381 (1998).
[7] F. Oosawa, Biopolymers **6**, 134 (1968).
[8] L. G. Gulbrand, Bo Jonsson, H. Innerstrom, and P. Linse, J. Chem. Phys. **80**, 2221 (1984).
[9] R. Kjellander, Ber. Bunsenges. Phys. Chem. **100**, 894 (1996).
[10] I. Rouzina and V. A. Bloomfield, J. Phys. Chem. **100**, 9977 (1996).
[11] N. Gronbech-Jensen, R. J. Mashl, R. F. Bruinsma, and W. M. Gelbart, Phys. Rev. Lett. **78**, 2477 (1997).
[12] B. J. Ha and A. J. Liu, Phys. Rev. Lett. **79**, 1289 (1997); *ibid.* **81**, 1011 (1998).
[13] R. Podgornik and V. A. Parsegian, Phys. Rev. Lett. **80**, 1560 (1998).
[14] J. J. Arenzon, J. F. Stilck, and Y. Levin, cond-mat/9806358.
[15] B. I. Shklovskii, Phys. Rev. Lett. **82**, 3268 (1999).
[16] V. I. Perel and B. I. Shklovskii, cond-mat/9902016, Physica A (1999).
[17] B. I. Shklovskii, cond-mat/9907351; Phys. Rev. E (1999).
[18] G. S. Manning, J. Chem. Phys. **51**, 924 (1969).
[19] B. Zimm and M. LeBret, J. Biomol. Struct. Dyn. **1**, 461 (1983).
[20] S. Leikin, A. A. Kornyshev, Phys. Rev. Lett. **82**, 4138 (1999).
[21] D. Rau and A. Parsegian, Biophys. J. **61**, 246 (1992).
[22] S. A. Safran, *Statistical Thermodynamics of Surfaces, Interfaces and Membranes*, Section 5.5 (Addison-Wesley, New York, 1994).
[23] L. D. Landau and E. M. Lifshitz, *Electrodynamics of Continuous Media* (Oxford-Pergamon, New York, 1998), Chap. 1.
[24] G. S. Manning, Biophys. Chem. **7**, 95 (1999).
[25] R. W. Wilson and V. A. Bloomfield, Biochemistry **18**, 2192 (1999).